Diagnosing the Intercept Parameter for Exponential Raindrop Size Distribution Based on Video Disdrometer Observations: Model Development

Guifu Zhang[1], Ming Xue[1,2], Qing Cao[1] and Daniel Dawson[1,2]
[1]School of Meteorology and [2]Center for Analysis and Prediction of Storms
University of Oklahoma

Submitted to J. Applied Meteorology and Climatology

September 2007

Corresponding author address:
Dr. Guifu Zhang
School of Meteorology
University of Oklahoma
120 David L. Boren Blvd, Suite 5900
Norman, OK 73072, USA
E-mail: guzhang1@ou.edu

Abstract

The exponential distribution $N(D) = N_0 \exp(-\Lambda D)$ with a fixed intercept parameter N_0 is most commonly used to represent raindrop size distribution (DSD) in rainfall estimation and in single-moment bulk microphysics parameterization schemes. Disdrometer observations show that the intercept parameter is far from constant and systematically depends on the rain type and intensity. In this study, a diagnostic relation of N_0 as a function of rain water content (W) is derived based on Two-Dimensional Video Disdrometer (2DVD) measurements. The data reveal a clear correlation between N_0 and the rain water content (W) where N_0 increases as W increases. To minimize the effects of sampling error, a relation between two middle moments is used to derive the $N_0 - W$ relation. This diagnostic relation has the potential to improve rainfall estimation and bulk microphysics parameterizations. A parameterization scheme for warm rain processes based on the diagnostic N_0 is formulated and presented. The diagnostic N_0-based parameterization yields less evaporation and accretion than the fixed N_0 model for stratiform rain.

1. Introduction

Information about the drop size distribution (DSD) is essential for understanding precipitation physics, estimating rainfall, and improving microphysics parameterizations in numerical weather prediction (NWP) models (Steiner et al. 2004). The characteristics of rain DSDs are often associated with the types of storms (e.g., convective versus stratiform rain) and their stages of development (e.g., the developing versus decaying stage, Brandes et al. 2006). Strong convective rain usually contains both large and small drops and has a broad DSD while the decaying stage is often dominated by small drops. Stratiform rain usually contains relatively larger drops but has a low number concentration for a given rain rate (Zhang et al. 2006).

Rain DSDs are usually represented by distribution models such as the exponential distribution, gamma distribution, and lognormal distribution. A DSD model usually contains a few free parameters that should be easy to determine and the model should be capable of capturing the main physical processes and properties. The exponential distribution is the most commonly used DSD model that has some of these properties, and it is given by

$$N(D) = N_0 \exp(-\Lambda D) . \qquad (1)$$

It contains two free parameters, N_0 and Λ. A single-moment bulk microphysics model predicts one of the moments of the DSD which determines one of the two parameters. The intercept parameter N_0 is usually specified so that Λ is uniquely related to the predicted water content, W, which in turn is linearly related to the 3rd moment of the DSD. The Marshall−Palmer (M-P, Marshall and Palmer 1948) exponential DSD model with the N_0 value fixed at 8000 m^{-3} mm^{-1} = 8×10^6 m^{-4} is widely used for representing warm rain (Kessler 1969) as well as ice (e.g., Lin et al. 1983; Hong et al. 2004) microphysics.

However, disdrometer observations and numerical model simulations indicate that N_0 and number concentration (N_t) are not constant, but vary depending on precipitation type, rain intensity and stage of development (Seifert, 2005). Waldvogel (1974) found large changes in N_0 for DSDs at different heights in profiling radar data. Sauvageot and Lacaux (1995) showed variations of both N_0 and Λ from impact disdrometer measurements. Recent observations by 2D Video Disdrometers (2DVD) suggest that rain DSDs are better represented by a constrained Gamma distribution (Zhang et al. 2001) that also contains two free parameters. In Zhang et al. (2006), the constrained Gamma model was further simplified to a single parameter model for bulk microphysical parameterization and the model produced more accurate precipitation system forecasts than the M-P model. Since the exponential distribution model is widely used, a diagnostic relation of N_0 as a function of W would improve rain estimation and microphysical parameterization that are based on such an improved model. Thompson et al. (2004) proposed a diagnostic N_0 relation using a hyperbolic tangent function to represent drizzle-type rain for winter weather prediction, which has not been verified by observations. The relation yields too many small drops and hence too much evaporation, which may not be applicable to summer time convection or stratiform rain types.

In this study, we derive a diagnostic N_0 relation from rain DSD data that were collected in Oklahoma using disdrometers. To minimize the error effects introduced in the fitting procedure, we formulate the problem with a relation between two DSD moments. A diagnostic relation is found from the relation between two middle moments. Section 2 describes methods of deriving the diagnostic relation and section 3 presents results of diagnosing N_0 from water content using 2DVD measurements. In Section 4, we discuss applications of the diagnostic relation in the parameterization of rain physics and microphysical processes. Final summary and discussions are given in section 5.

2. Diagnosing methods

The diagnostic relation for the intercept parameter N_0 as a function of water content can be derived using two different approaches: (i) direct fitting approach and (ii) moment relation method, described as follows.

The Direct Fitting Approach (DFA) is to first find the DSD parameters (N_0, Λ) by fitting DSD (e.g., disdrometer) data to the exponential function (1) for each DSD, and then plot the estimated N_0 versus W for the whole dataset for fitting a mean relation.

The nth moment of the exponential DSD (1) is

$$M_n = \int D^n N(D) dD = N_0 \Lambda^{-(n+1)} \Gamma(n+1) \quad . \tag{2}$$

Hence, the DSD parameters, N_0 and Λ, can be determined from any two moments (M_l, M_m) as

$$\Lambda = \left(\frac{M_l \Gamma(m+1)}{M_m \Gamma(l+1)} \right)^{\frac{1}{m-l}}, \tag{3}$$

$$N_0 = \frac{M_l \Lambda^{l+1}}{\Gamma(l+1)}. \tag{4}$$

When N_0 is obtained along with the water content W for DSD data sets, a $N_0 - W$ relation can be found through another fitting procedure, e.g., the power-law fitting. It is noted that the values of the estimated N_0 depend on which two moments are used and on the accuracy of the two moment estimates. Since the estimates of both the moments (M_l, M_m) have error, the DSD parameters (N_0, Λ) obtained from them will also have error. The natural variation in DSDs also causes a large scatter in the $N_0 - W$ plot (see Fig. 2 in next section). The estimation error and natural variation are very difficult to separate unless two or more instruments are used (Cao et al. 2007) Hence, the $N_0 - W$ relation derived from the above procedure tends to have larger errors.

To minimize the error effects introduced in the fitting procedures, we propose an alternative method, called Moment Relation Method (MRM), for obtaining the $N_0 - W$ relation. In MRM, we first seek to establish a relation between two DSD moments. With this relation, the exponential distribution is reduced to having a single free parameter so that N_0 can be determined from W. Suppose that two DSD moments M_l, and M_m are related by a power-law relation:

$$M_l = aM_m^b, \tag{5}$$

where a and b are coefficients that can be estimated from disdrometer observations.

From Eq. (2) for the third moment, we have water content $W = \frac{\pi}{6}\rho M_3 = \pi\rho N_0 \Lambda^{-4}$, [$\rho$ is water density], yielding the slope parameter $\Lambda = \left(\frac{N_0 \pi \rho}{W}\right)^{1/4}$. Substituting (2) into (5) for M_l and M_m, and making use of the relation for Λ, we obtain

$$N_0 = \alpha W^{\beta}, \tag{6}$$

where

$$\alpha = \left(a \frac{\Gamma^b(m+1)}{\Gamma(l+1)\pi^c \rho^c} \right)^{\frac{1}{1-b+c}}, \tag{7}$$

$$\beta = \frac{c}{1-b+c}, \tag{8}$$

and

$$c = \frac{b(m+1) - (l+1)}{4}. \tag{9}$$

Hence, (6) - (9) constitute a general formulation for deriving a $N_0 - W$ relation using a statistical relation between two DSD moments. When the coefficients a and b in the relation (5) are determined from a set of DSD data, we have a diagnostic relation between the water content W and

the intercept parameter N_0. This is the procedure that will be used in the next section with a disdrometer dataset.

3. Derivation of the $N_0 - W$ relation from disdrometer observations

We test our method for deriving the $N_0 - W$ relation using disdrometer data collected in Oklahoma during the summer seasons of 2005, 2006 and 2007 (Cao et al. 2007). Three 2DVDs, operated respectively by the University of Oklahoma (OU), National Center for Atmospheric Research (NCAR) and National Severe Storms Laboratory (NSSL) were deployed at the NSSL site in Norman, Oklahoma, and at the Southern Great Plains (SGP) site of the Atmospheric Radiation Measurement (ARM) program. The ARM site is located approximately 28 km south of the NSSL site. A total of 14200 minutes of disdrometer data with total drop counts greater than 50 were collected. Among them are 435 minutes of data that have side-by-side measurements by two 2DVDs. The recorded raindrops within each minute were processed to produce one-minute DSD samples, yielding a total of 14200 DSDs.

With the side-by-side data, measurement errors of DSDs were quantified. The sampling errors are further reduced by sorting and averaging based on two parameters (SATP), a method that combines DSDs with similar rainfall rates (R) and median volume diameters (D_0) (Cao et al. 2007). There are 2160 quality-controlled DSDs after SATP processing for the dataset. The DSD moments are estimated by the sum of weighted DSDs as defined in (2). As shown in Table 1 of Cao et al. (2007), the relative errors of the moments: M_0, M_2 M_3, M_4 and M_6 are: 10.3, 9.1, 9.0, 10.3, and 17.5%, respectively. In addition, the low moment measurements are highly affected by wind, splashing and instrumentation limits, resulting in even more error that is not shown in that table. Since the middle moments (M_2 M_3, M_4) are measured more accurately, their use in DSD

fitting should be more reliable. It is dersiable to consider both error effect and physical significance of the moments being used for the application. A moment pair (M_2, M_4) is considered a good combination that balances them both well.

As example, three measured rain DSDs are shown in Fig. 1 as discrete points. They correspond to strong convection, weak convection and stratiform rain, respectively, taken from the rain events shown in Figs. 5c and 6c. Using the moment pair of (M_2, M_4), the DSDs are fitted to the exponential distribution, shown as dashed lines. The exponential DSD model fits data reasonably well, especially for strong convection. But it does not capture the curvature shape of the natural DSDs and tend to overestimate number concentration for stratiform and weak convective rain. It is clear the intercept N_0 are quiet different, but there seems a systematic/statistical trend: the heavier the rain intensity, the larger the N_0 value.

The exponential DSD parameters N_0 and Λ are estimated from the moment pairs of (M_0, M_3), (M_2, M_4), and (M_3, M_6) using Eqs. (3) and (4) for the whole dataset. The exponentially-fitted N_0 values are plotted versus the rain water content in Fig. 2. As expected, there is a large scatter in the $N_0 - W$ plot because of measurement and model errors as well as natural variations. It is important to note that the N_0 variability is part of rain microphysical properties, represented by the exponential DSD model. Also, different moment pairs produce different results of N_0 due to differences in estimation error and error propagation in the fitting procedure (Zhang et al. 2003). It is clear that there is a positive correlation between N_0 and W. However, due to the large scatter of data points in Fig. 2, it is difficult to fit them to stable $N_0 - W$ relations. For example, minimizing error in the x-axis (W) gives a different result from that of minimizing error in the y-axis (N_0). We chose to minimize the errors on both axes, yielding the results shown in Fig. 2 as straight lines.

The coefficients (α, β) for these power-law relations are listed in Table 1. As discussed earlier, the most reliable result is that from the pair (M_2, M_4), which is

$$N_0^{(D)}(M_2, M_4) = 24144W^{1.326}. \quad (10)$$

Even after minimizing errors on both axes, the results are not optimized, due to the large scatter of the data.

Instead, an $N_0 - W$ relation is derived from a moment relation as outlined in section 2. Figure 3 shows the scatter plots of moments for the pair of (M_0, M_3), (M_2, M_4) and (M_3, M_6) directly calculated from the DSD data, and the corresponding power-law relations are obtained as

$$M_0 = 0.962M_3^{1.040}, \quad (11a)$$

$$M_2 = 1.473M_4^{0.838}, \quad (11b)$$

$$M_3 = 3.038M_6^{0.626}. \quad (11c)$$

For the moment pair (M_2, M_4), we have a = 1.473 and b = 0.838 in Eq.(5). The correlation between the moments is high, with a correlation coefficient of 0.85 in the linear domain and 0.90 in the logarithmic domain for this pair. Substituting for a and b in (6)-(9), we obtain α = 7106 and β = 0.648, therefore

$$N_0^{(M)}(M_2, M_4) = 7106W^{0.648}. \quad (12)$$

The results with the other moment pairs of (M_0, M_3) and (M_3, M_6) are shown in Table 1 with their coefficients. This N_0 - W relation (12) derived from the moment pair (M_2, M_4) is shown in Fig. 4 along with those derived from moment pairs (M_0, M_3) and (M_3, M_6) as thick lines. The lower (higher) moment pair yields a relation with a larger (smaller) slope, which is opposite to the DFA results. Overall, the DFA results have even bigger slope, attributed to the error effects of small number of drops for light rain. Nevertheless, they all have increase trend with W. The diagnostic relation by Thompson et al. (2004) is also shown for comparison, which has opposite

trend as those developed here based on disdrometer data. Hence, Thompson's relation proposed for winter weather drizzle may not apply to convective and stratiform rain events.

As discussed earlier, the middle moment pair (M_2, M_4) has smaller errors and its derived relations should be used. The two N_0 - W relations: (10) and (12), derived using the DFA and MRM methods, and the fixed N_0 are compared by through their error statistics. The mass-weighted relative absolute error of moment estimates using the constrained exponential DSD models is calculated as

$$\gamma_n = \frac{\sum_{l=1}^{L} \left| M_n^{(e)}(l) - M_n^{(m)}(l) \right| \times M_3^{(m)}(l)}{\sum_{l=1}^{L} M_n^{(m)}(l) \times M_3^{(m)}(l)}, \qquad (13)$$

where the measured n^{th} moment is $M_n^{(m)}(l)$ that is directly calculated from the l^{th} DSD, $M_n^{(e)}(l)$ is the estimated moment from water content using the diagnostic N_0 DSD model. The results are listed in Table 2. It is shown that the DFA relation (10) yield larger errors, with negative biases for the higher moments (M_4, M_5, and M_6) , and positive biases for the lower moments (M_0, M_1, and M_2). This is because the DFA treats each data point with equal weight in the log-log plot (Fig. 2). The large number of light rain DSDs may dominate the fitted relation, leading an unrealistically large power coefficient and yielding over (under) estimation of N_0 for heavy (light) rain, and hence the negative and positive biases. However, the moment errors with relation (12) are much smaller, especially for the lower moments, because the MRM-derived relation accounts for proper weighting. It is interesting to note that the fixed-N_0 M-P model performs better than the DFA-derived relation. This shows the importance of the procedure used in deriving a diagnostic relation. It is obvious that the MRM relation (12) has the best performance in characterizing rain microphysics. Therefore relation (12) is recommended.

For a better understanding of the $N_0 - W$ relation (12), Figure 5 shows an example of N_0 values along with other physical parameters (N_t, W, and D_0) as a function of time for a convective rain event starting on July 21, 2006. It was a strong convective storm followed by weak convections passing over the OU disdrometer deployed at the ARM site at Washington, Oklahoma. The water content is very low during the weak convection periods, but the median volume diameter D_0 is comparable to that of strong convection. The comparison between exponentially-fitted N_0 values from DSD moments M_2 and M_4 and those diagnosed from W using (12) is plotted in Fig. 5a. Had the Thompson's (2004) relation been plotted, it would have been out of the range except for the strong convection period. As shown in Fig. 5b, the moment fitting of the exponential DSD model yields a good estimate of total number concentration N_t as compared with the direct estimates from DSD data (discrete "+"). Here, the fitted N_0 can be considered as "truth" because N_0 is a model parameter which is obtained through the fitting procedure of Eqs. (2) - (4). It is clear that the diagnosed N_0 captures the main trend of the observed rain storm very well in a dynamic range of more than two orders of magnitude; that is, from an order of 10^4 for strong convention to 10 for light rain precipitation. In comparison, the fixed-N_0 M-P model overestimates N_0 except for heavy convective rain. Figure 5d compares median volume diameter D_0 calculated from the DSD data, estimated using the diagnostic-N_0 model and that with the fixed-N_0 model.

Figure 6 shows the same parameters as that in Fig. 5, but for a convection-ticked stratiform rain event started on November 6, 2006. Again, the diagnostic $N_0 - W$ relation produces a much better agreement with the measurements than does the fixed-N_0 model. It is noted that the stratiform rain (after 2230 UTC) has a much low number concentration (N_t<500). Even the exponential fit and the diagnostic N_0 model overestimate N_t by three to four times. This is because stratiform rain DSDs tend to have a convex shape and do not contain many small drops as the

exponential model has. Also, since the dataset are dominated by convective rain events and the derived relation (12) may not represent stratiform rain as good as the convective rain. Further reduction of N_0 may be needed for better representing stratiform rain characteristics.

4. Application to warm rain microphysical parameterization

The warm rain microphysical processes related to the DSD include rain evaporation, accretion of cloud water by rain water, and rain sedimentation. The microphysical parameters of these processes based on the exponential DSD model have been derived by Kessler (1969: Table 4). After unit conversion, the evaporation rate (R_e in kg kg^{-1} s^{-1}), accretion rate (R_c in kg kg^{-1} s^{-1}), mass-weighted terminal velocity (V_{tm} in m s^{-1}), and reflectivity factor (Z in mm^6 m^{-3}) are given by

$$\mathrm{R_e} = 2.17\times10^{-5} E_e N_0^{7/20}(q_{vs}-q_v)\mathrm{W}^{13/20}, \tag{14a}$$

$$\mathrm{R_c} = 1.65\times10^{-3} E_c N_0^{1/8} q_c \mathrm{W}^{7/8}, \tag{14b}$$

$$\mathrm{V_{tm}} = 16.4 N_0^{-1/8} W^{1/8}\left(\rho_0/\rho\right)^{0.5}, \tag{14c}$$

$$\mathrm{Z} = 1.73\times10^{7} N_0^{-3/4} W^{7/4}. \tag{14d}$$

where E_e and E_c are the evaporation and accretion efficiency factors, respectively (normally taken as 1), W is rain water content in g m^{-3} as before ($W = 1000\rho q_r$), q_v, q_c and q_r are, respectively, the water vapor, cloud water and rain water mixing ratios in kg kg^{-1}.

Substituting the diagnostic relation (12) into (14) and assuming unit saturation deficit and unit cloud water mixing ratio as well as unit efficiency factors, we obtain a parameterization scheme based on the diagnostic N_0. The terms corresponding to those in Eq. (14) are listed in Table 3 along with those of the standard fixed-N_0 M-P model. The coefficients of these terms are similar for the two schemes, but the powers are substantially different. The larger power in evaporation rate means more (less) evaporation for heavy (light) rain compared to the fixed-N_0 model. The

smaller power in the reflectivity formula for the diagnostic-N_0 model gives smaller (larger) reflectivity than the fixed N_0 for heavy (light) rain. This may lead to a better agreement between numerical model forecasts and radar observations. The former tends to over-predict large reflectivity values and under-predict low reflectivity values. In this sense, the diagnostic-N_0 model has similar properties as the simplified-constrained-gamma model investigated in Zhang et al. (2006).

Figure 7 compares the two parameterization schemes based on the diagnostic-N_0 and fixed-N_0 DSD models, respectively, by showing the microphysical processes/parameters as a function of W. The direct calculations from the DSD dataset are also shown for comparison. The diagnostic-N_0 results agree well with that from the measurements except for the calculated reflectivity. As stated in the previous paragraph, the diagnostic-N_0 model yields smaller (larger) evaporation and accretion rates for light (heavy) rain than the fixed-N_0 model. However, the diagnostic-N_0 model gives large (small) reflectivity and mass-weighted velocity values for light (heavy) rain cases. It is noted that the low end of the data points in Fig. 7b are associated with light rain and have large sampling errors. The performance of the DSD models should also be evaluated by calculating the relative errors for all the moments, as given in Table 2 and discussed earlier.

Figure 8 and 9 compare the terms for the microphysical processes estimated from W using the diagnostic-N_0 DSD model with those from the fixed-N_0 M-P DSD model for the two rain events shown in Figs. 5 and 6. Direct calculations from the observed DSD data and those fitted with the exponential model with N_0 as one of the two free parameters are also shown for reference. The results may appear to be close to each other in the semi-logarithm plots but actually, the fixed-N_0 model overestimates the evaporation rate for stratiform rain by about a factor of five and underestimates that for strong convection. This might be the reason that the parameterization

coefficients in the Kessler scheme are sometimes reduced by a half and more in order to obtain a better match of modeling results with observations (e.g., Miller and Pearce 1974; Sun and Crook 1997). The diagnostic-N_0 model therefore characterizes rain evaporation, accretion and rainfall processes more accurately than the fixed-N_0 model for both heavy and light rainfall. By introducing the dependency of N_0 on W based on observations, raindrop number concentration and total surface area of rain drops are better represented, leading to a better estimation of evaporation and accretion rates.

5. Summary and Discussions

In this paper, we present a method for diagnosing the intercept parameter N_0 of the exponential drop size distribution (DSD) based on water content W, and apply the diagnostic-N_0 DSD model towards improving warm rain microphysical parameterization. The diagnostic relation is derived from a relation between two DSD moments that are estimated from 2D video disdrometer data. The DSD data were collected in Oklahoma during the summer seasons of 2005 and 2006, which should be representative for rains in the central Great Plains region. The diagnostic $N_0 - W$ relation is used to improve the Kessler parameterization scheme of warm rain microphysics, and can be used in schemes containing ice-phases also (e.g., those in commonly used schemes of Lin et al. 1983 and Hong et al. 2004).

It has been shown that the diagnostic-N_0 model better characterizes natural rain DSDs, including the physical properties (e.g., N_t, and D_0) and microphysical processes. For a given water content, the diagnostic-N_0 DSD model represents the total number concentration, median volume diameter, reflectivity factor, evaporation rate and accretion rate much more accurately than the M – P model with a fixed N_0. Compared with the M-P model-based Kessler scheme, the

modified parameterization scheme with a diagnostic N_0 has the following advantages: (i) it leads to less (more) evaporation for light (heavy) rain and therefore can preserve stratiform rain better in numerical models, and (ii) it yields a larger (smaller) reflectivity factor for light (heavy) rain, having the potential of yielding a better agreement between model predicted and radar observed reflectivities in a similar way as the simplified constrained gamma model. Realistic simulation of reflectivity is important for assimilating radar reflectivity data into NWP models.

It is noted that the diagnostic $N_0 - W$ relation obtained in this paper is based on a specific set of disdrometer data in a specific climate region, dominated by convection rain events. While the methodology developed in this paper is general, the coefficients in the relation may need to be tuned to better fit specific regions and/or seasons or specific rain types. For example, the coefficient of (12) may need to be reduced by a factor of two to three to better represent stratiform rain characteristics. The improved parameterization based on the diagnostic-N_0 model is now being tested within a mesoscale model for real events to examine its impact on precipitation forecast; the results will be presented in the future.

*Acknowledgments***.** Authors greatly appreciate helps from Drs. Edward Brandes, Terry Schuur, Robert Palmer, Phillip Chilson and Ms. Kyoko Iketa. The sites for disdrometer deployment at the Kessler farm were provided by Atmospheric Radiation Measurement (ARM) Program. This work was primarily supported by a NSF grant ATM-0608168. Ming Xue and Dan Dawson were also supported by NSF grants ATM-0530814, ATM-0331594 and ATM-0331756.

References

Brandes, E. A., G. Zhang, and J. Vivekanandan, 2002: Experiments in rainfall estimation with a polarimethic radar in a subtropical environment. *J. Appl. Meteor.,* **41,** 674-685.

Brandes, E. A., G. Zhang, and J. Sun, 2006: On the influence of assumed drop size distribution form on radar-retrieved thunderstorm microphysics. *J. Appl. Meteor*, 45, 259-268,

Cao, Q., G. Zhang, E. Brandes, T. Schuur, A. Ryzhkov, and K. Ikeda, 2007: Analysis of video disdrometer and polarimetric radar data to characterize rain microphysics in Oklahoma. *J. Appl. Meteor. Climat. Under review.*

Hong, S.-Y., J. Dudhia, and S.-H. Chen, 2004: A revised approach to ice microphysical processes for the bulk parameterization of clouds and precipitation. *Mon. Wea. Rev.,* **132,** 103–120.

Kessler, E., 1969: On the distribution and continuity of water substance in atmospheric circulations. *Meteor. Monogr.,* No. 32, Amer. Meteor. Soc., 84 pp.

Lin, Y.-L., R. D. Farley, and H. D. Orville, 1983: Bulk parameterization of the snow field in a cloud model. *J. Climate Appl. Meteor.,* **22,** 1065−1092.

Marshall, J.S., and W. McK. Palmer, 1948: The distribution of raindrops with size, *J. Meteor*., **5**, 165-166.

Miller, M. J., and R. P. Pearce, 1974: A three-dimensional primitive equation model of cumulonimbus convection. *Quart. J. Roy. Meteor. Soc*., 100, 133–154.

Sauvageot, H., and J.-P. Lacaux, 1995: The shape of averaged drop size distributions. *J. Atmos. Sci*., **52**, 1070–1083.

Seifert A, 2005: On the shape-slope relation of drop size distributions in convective rain. *J. Appl. Meteor.*, **44** (7), 1146-1151.

Smith, P. L., and D. V. Kliche, 2005: The Bias in Moment Estimators for Parameters of Drop Size Distribution Functions: Sampling from Exponential Distributions, *J. Appl. Meteor*., **44**, 1195–1205.

Steiner, M., J. A. Smith, and R. Uijlenhoet, 2004: A microphysical interpretation of radar reflectivity-rain rate relationships. *J. Atmos. Sci.*, **61**, 1114-1131.

Sun, J, and N. A. Crook, 1997: Dynamical and microphysical retrieval from Doppler radar observations using a cloud model and its adjoint. Part I: Model development and simulated data experiments. *J. Atmos. Sci*., 54, 1642–1661.

Thompson, G., R. M. Rasmussen, and K. Manning, 2004: Explicit forecasts of winter Precipitation using an improved bulk microphysics scheme. Part I: Description and Sensitivity Analysis, *Mon. Wea. Rev*., **132**, 519-542

Waldvogel, A., 2006: The N_0 Jump of raindrop Spectra. *J. Atmos. Sci.***, 31**, 1067-1078.

Zhang, G., J. Vivekanandan, and E. Brandes, 2001: A method for estimating rain rate and drop size distribution from polarimetric radar measurements. *IEEE Trans. Geosci. Remote Sens.,* **39,** 830–841.

Zhang, G., J. Vivekanandan, E.A. Brandes, R. Meneghini, and T. Kozu, 2003: The shape-slope relation in Gamma raindrop size distribution: statistical error or useful information?, *J. Atmos. Ocean. Tech*., **20**. 1106-1119.

Zhang, G., J. Sun, and E. A. Brandes, 2006: Improving parameterization of rain microphysics with disdrometer and radar observations. *J. Atmos. Sci.***, 63**, 1273-1290.

Figure captions

Fig. 1: Examples of raindrop size distributions and their fit to exponential distribution using the moment pair (M_2, M_4), The four DSDs correspond to strong convection, weak convection and stratiform rain.

Fig. 2: Dependence of intercept parameter (N_0) on water content (W). Scattered points are fitted results from a pair of DSD moments. Straight lines are derived relations using direct fitting method.

Fig. 3: Inter-relationships among DSD moments based on disdrometer measurements. Scattered points are direct estimates from disdrometer measurements. Straight lines represent fitted power-law relations. (a): M0-M3, (b): M2-M4, and (c): M3:M6.

Fig. 4: Results of diagnostic N_0-W relations using the moment relation method. The direct fitting method and Thompson et al results are shown for comparison.

Fig. 5: Time series comparison of physical parameters: intercept parameter (N_0), total number concentration (N_t) water content (W), and median volume diameter (D_0) for a convective rain event starting on July 21, 2006. Results are shown for disdrometer measurements and fitted values using exponential, diagnostic-N_0, and fixed-N_0 DSD models.

Fig. 6: As in Fig. 5 for a straitiform rain event on November 6, 2006.

Fig. 7: Comparison of rain physical process parameters for a unit saturation deficit and cloud water mixing ratio between the diagnostic N_0 and fixed DSD models. (a) R_e and R_c in kg kg^{-1} s^{-1}, and V_{tm} in m s^{-1}, and (b) reflectivity Z in mm^6 m^{-3}

Fig.8: As in Fig. 5 except for evaporation rate for a unit vapor saturation deficit (R_e), accretion rate (R_c) for a unit cloud water content, and mass-weighted terminal velocity (V_{tm})

Fig. 9: As in Fig. 7 for the stratiform rain event on November 6, 2006

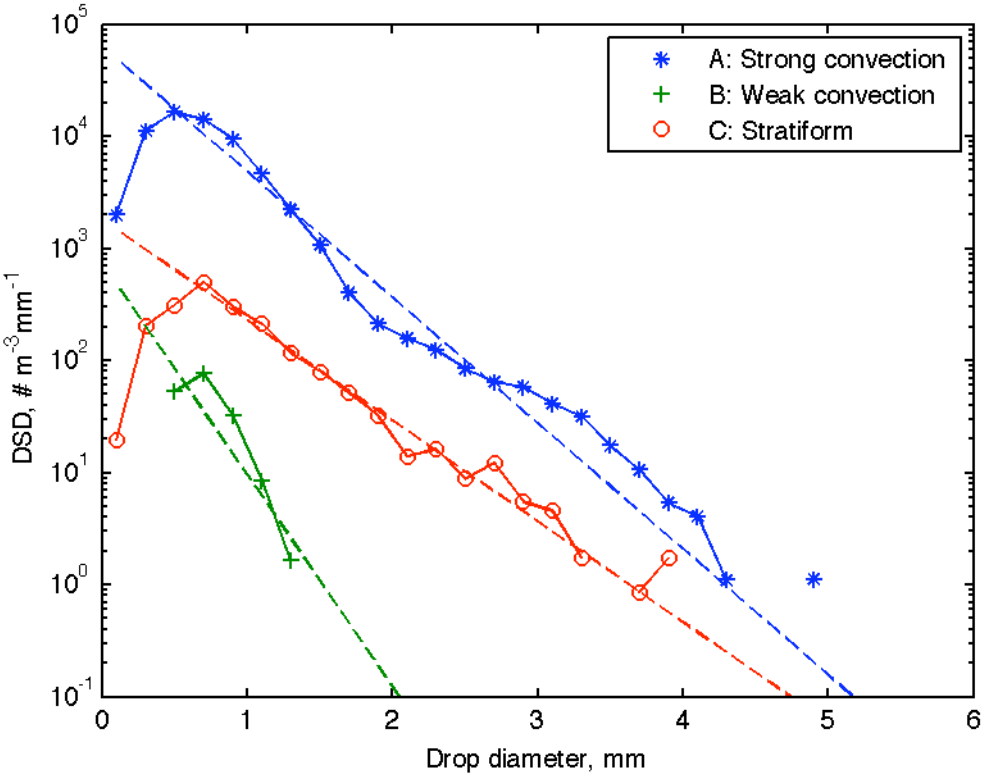

Fig. 1: Examples of raindrop size distribution and their fits to exponential distribution using the moment pair (M_2, M_4), The three DSDs correspond to strong convection, weak convection and stratiform rain.

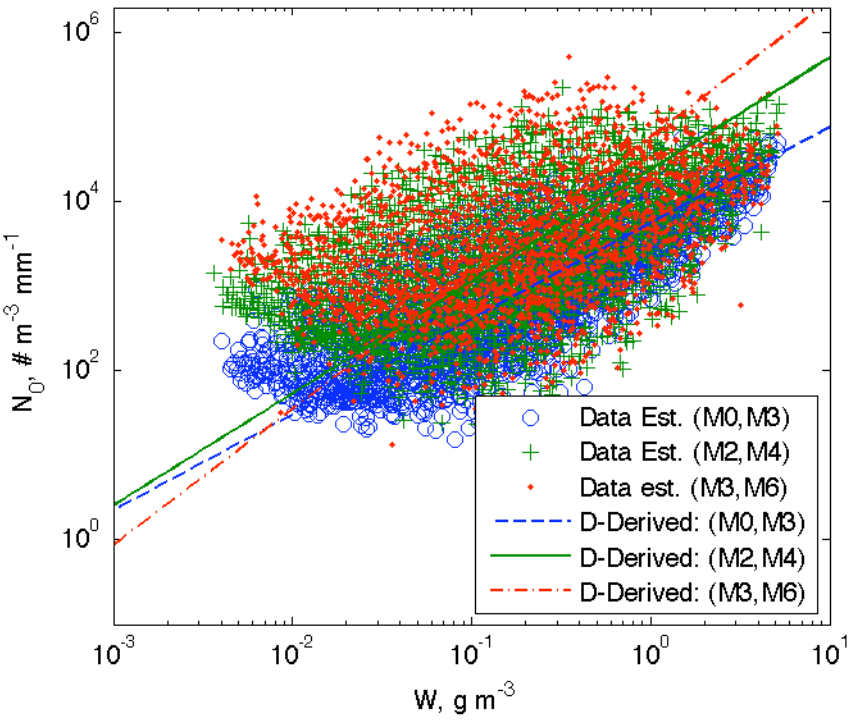

Fig. 2: Dependence of intercept parameter (N_0) on water content (W). Scattered points are fitted results from a pair of DSD moments. Straight lines are derived relations using direct fitting method.

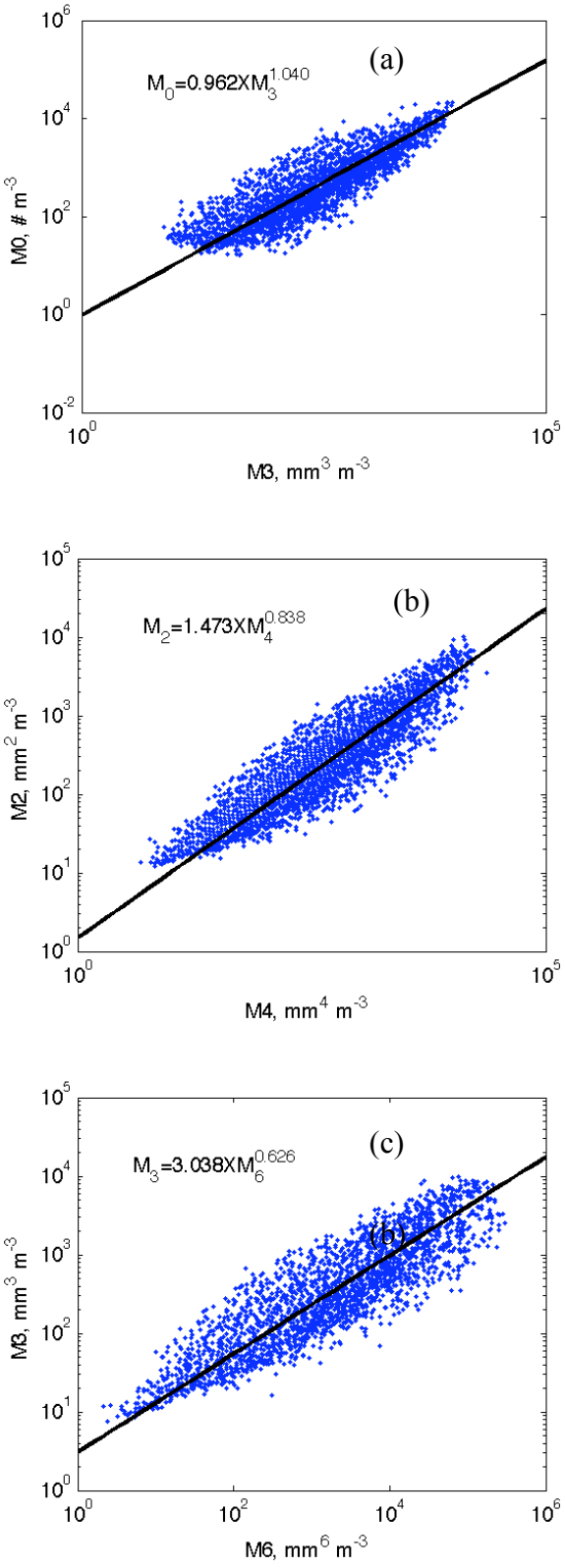

Fig. 3: Inter-relationships among DSD moments based on disdrometer measurements. Scattered points are direct estimates from disdrometer measurements. Straight lines represent fitted power-law relations. (a): M0-M3, (b): M2-M4, and (c): M3:M6.

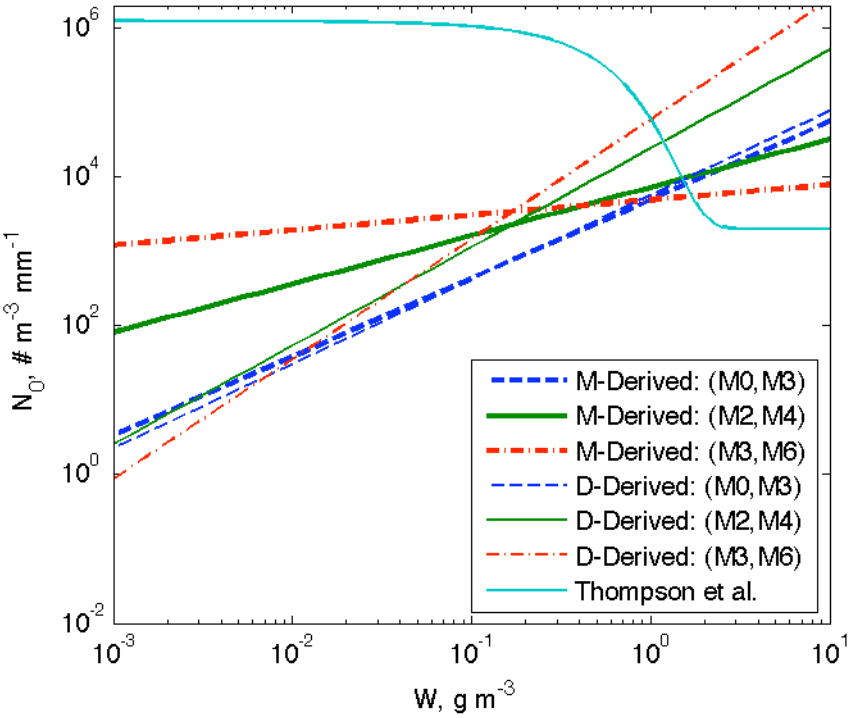

Fig. 4: Diagnostic N_0-W relations obtained using the moment relation method. The results of direct fitting approach and Thompson et al approach are shown for comparison.

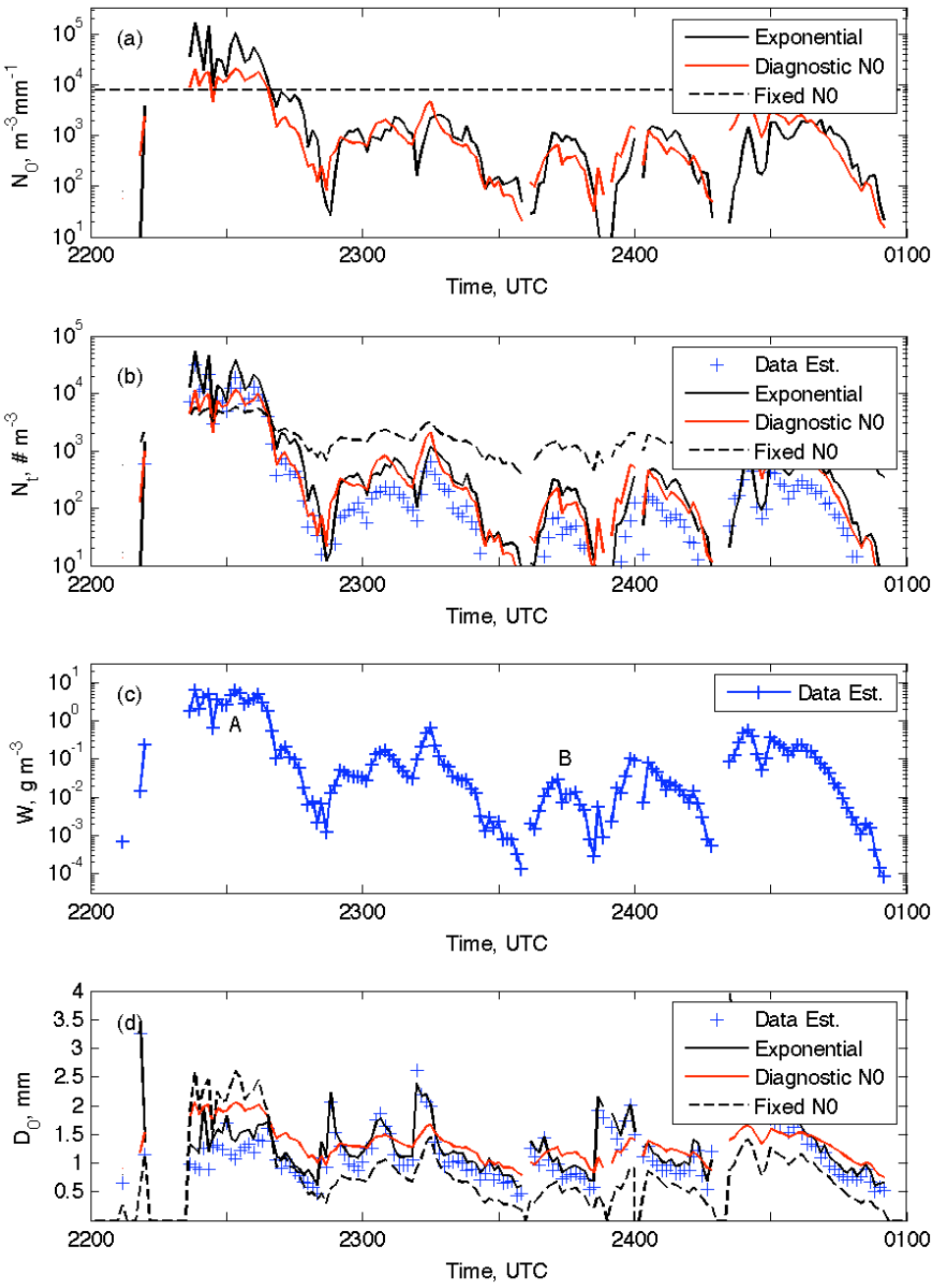

Fig. 5: Time series of intercept parameter (N_0), total number concentration (N_t), water content (W), and median volume diameter (D_0) for a convective rain event starting on July 21, 2006, for disdrometer measurements and fitted values using exponential, diagnostic-N_0, and fixed-N_0 DSD models.

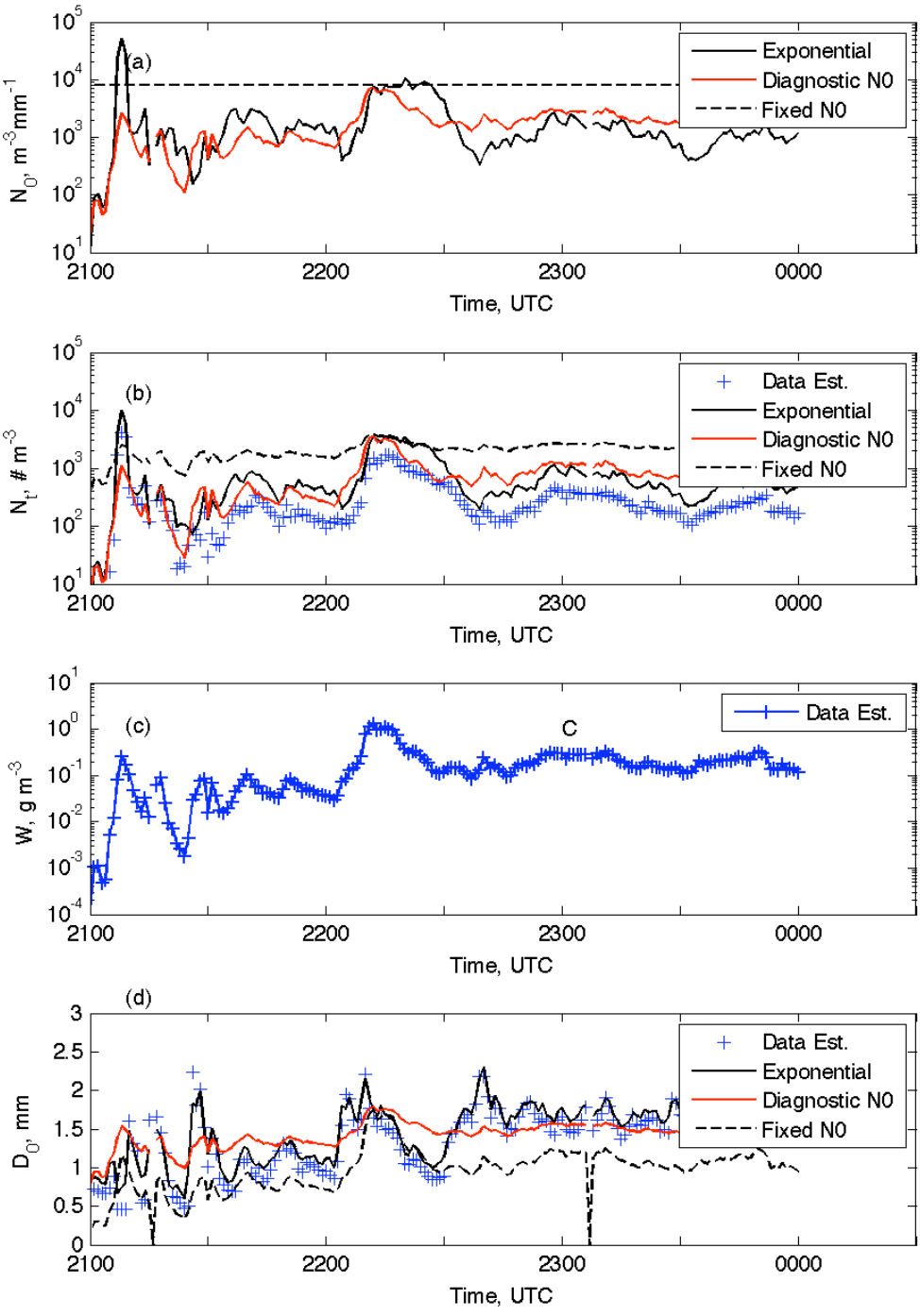

Fig. 6: As Fig. 5 for a stratiform rain event on November 6, 2006.

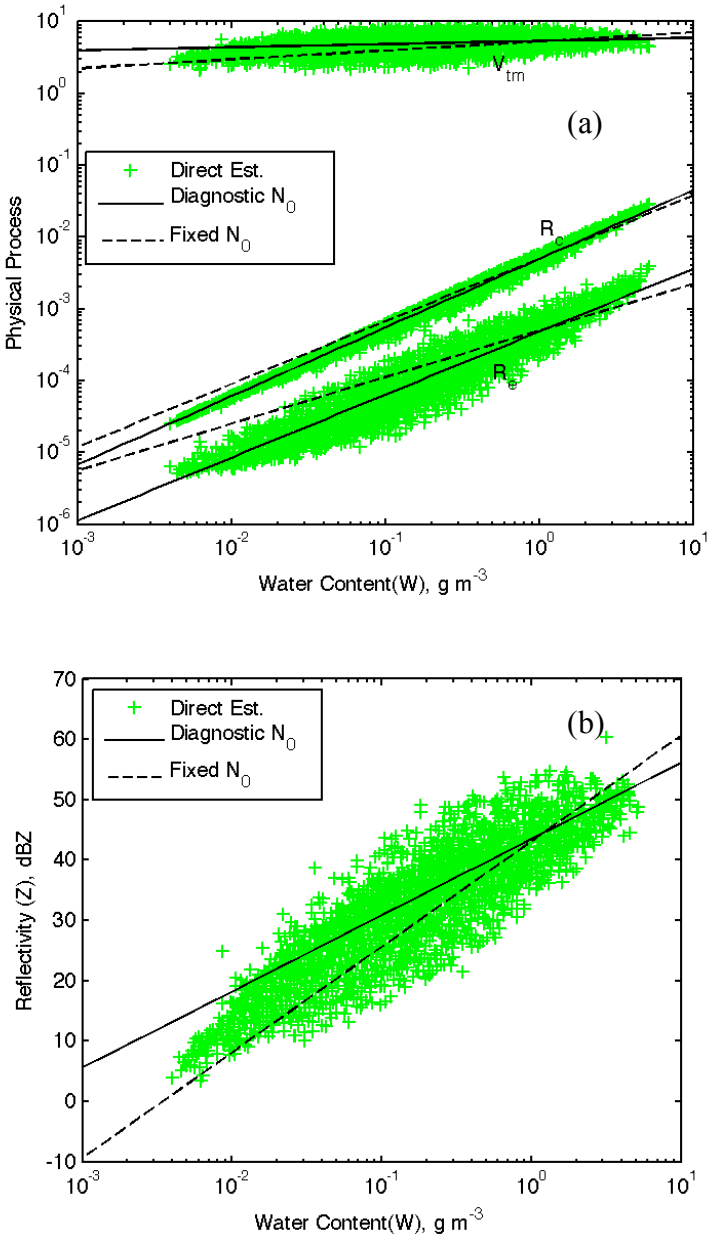

Fig. 7: (a) Rain evaporation rate R_e and accretion rate R_c in kg kg^{-1} s^{-1}, and terminal velocity V_{tm} in m s^{-1}, and (b) reflectivity Z in mm^6 m^{-3}, when calculated based on the diagnostic-N_0 and fixed-N_0 DSD models for a unit saturation deficit and unit cloud water mixing ratio.

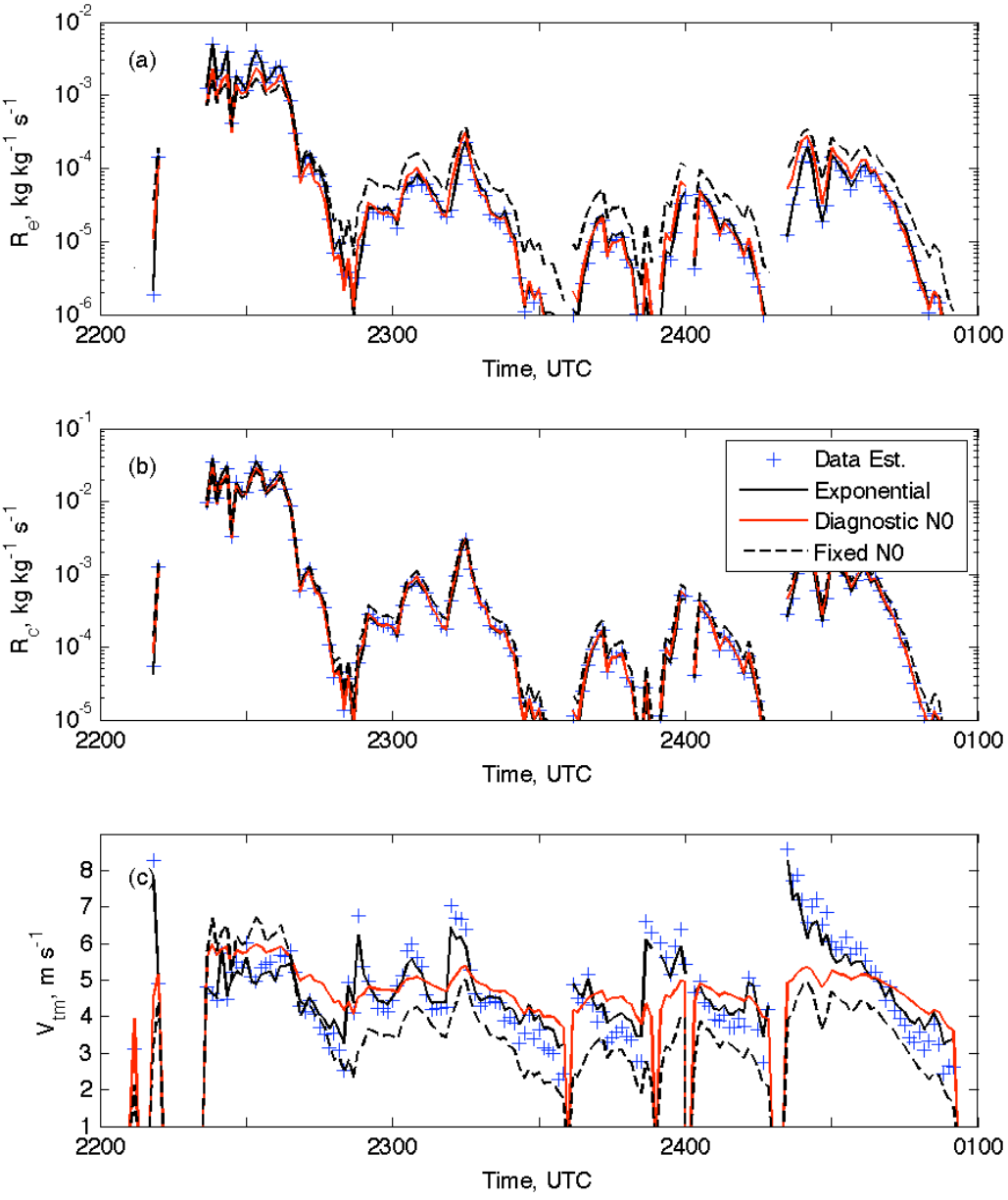

Fig.8: Rain evaporation rate (R_e) for a unit vapor saturation deficit (a), accretion rate (R_c) for a unit cloud water content (b), and mass-weighted terminal velocity (V_{tm}) (c), for a convective rain event starting on July 21, 2006, for disdrometer measurements and fitted values using exponential, diagnostic-N_0, and fixed-N_0 DSD models.

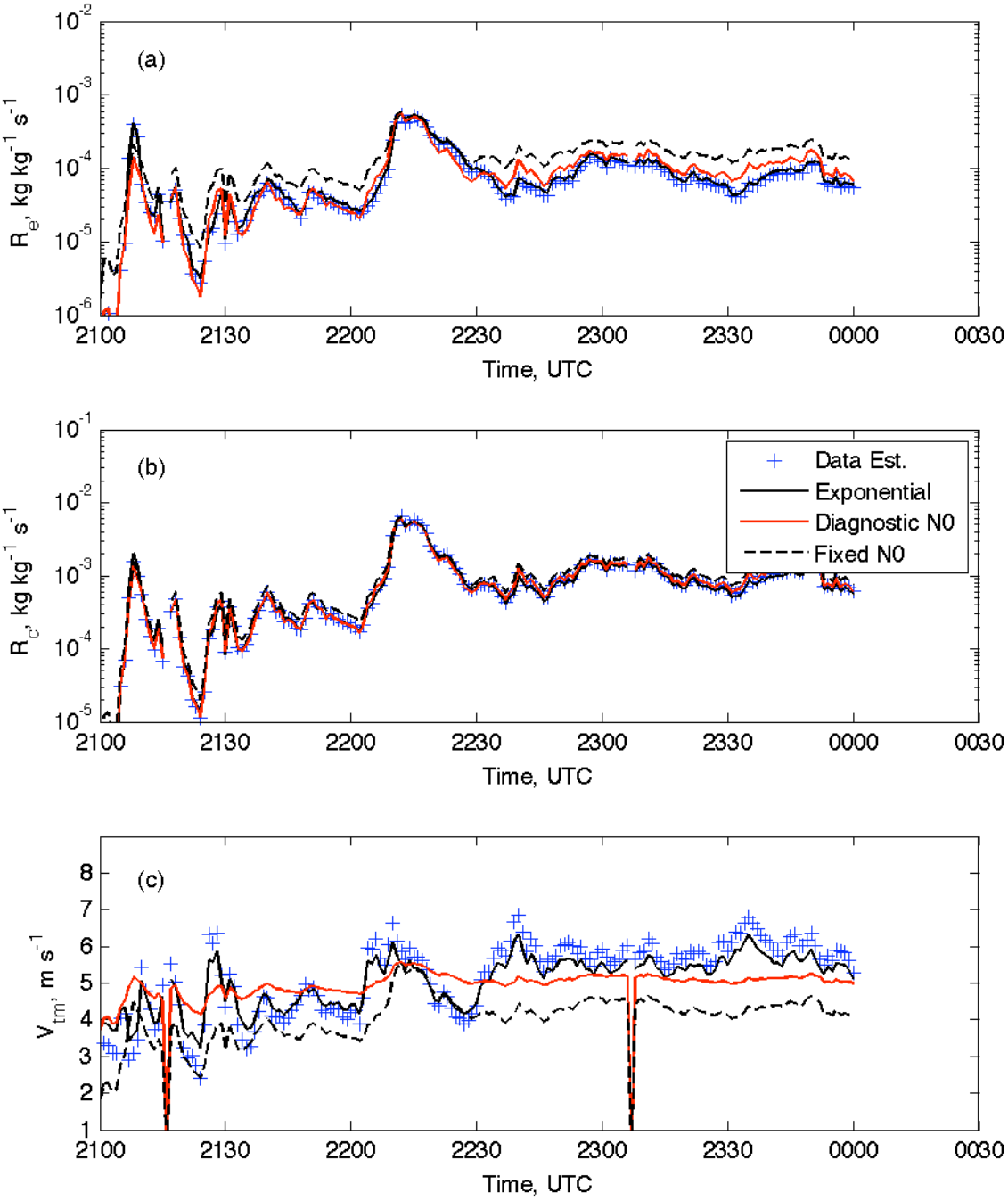

Fig. 9: As Fig. 8 but for the stratiform rain event on November 6, 2006

Table 1: Coefficients of diagnostic N_0-W relations

Moment pair	DFA		MRM	
	α	β	α	β
M_0, M_3	5674	1.135	4910	1.053
M_2, M_4	24144	1.326	7106	0.648
M_3, M_6	58842	1.611	4903	0.204

Table 2: Comparison of relative errors of moment estimates

Moment		M_0	M_1	M_2	M_3	M_4	M_5	M_6
γ_n, %	DFA: (10)	285.6	90.4	35.1	0.0	32.6	59.8	78.0
	MRM: (12)	41.9	34.9	21.9	0.0	24.4	45.3	62.5
	M-P: fixed N_0	59.3	47.9	29.6	0.0	35.9	69.5	97.0

Table 3: Parameterization of warm rain processes with diagnostic N_0 and fixed N_0

Parameterized quantity	Diagnostic N_0	Fixed N_0
N_0, m^{-3} mm^{-1}	$7106W^{0.648}$	8000
R_e, kg kg^{-1} s^{-1}	$4.84\times10^{-4}W^{0.878}$	$5.03\times10^{-4}W^{0.65}$
R_c, kg $kg^{-1}s^{-1}$	$5.0\times10^{-3}W^{0.956}$	$5.08\times10^{-3}W^{0.875}$
V_{tm}, m s^{-1}	$5.41W^{0.044}$	$5.32W^{0.125}$
Z, mm^6 m^{-3}	$2.24\times10^{4}W^{1.264}$	$2.04\times10^{4}W^{1.75}$